Available online at http://scik.org
J. Math. Comput. Sci. 2023, 13:13
https://doi.org/10.28919/jmcs/8149
ISSN: 1927-5307

# MATHEMATICAL ANALYSIS OF THE RESOLUTION OF THE SALTWATER INTRUSION PROBLEM IN A COASTAL AQUIFER USING THE RBF COLLOCATION METHOD

ANTOINE FILANKEMBO OUASSISSOU[1], CORDY JOURVEL ITOUA-TSELE[1,2,*], CHRISTIAN TATHY[2], DEN JUSTICE MATOUADI[1]

[1]Department of Exact Sciences, Higher Teacher's Training School, Marien Ngouabi University, Brazzaville, Congo

[2]Laboratory of Mechanics Energy and Engineering, Higher National Polytechnics School, Marien Ngouabi University, Brazzaville, Congo



**Abstract.** Contamination of drinking water sources can result from the issue of saltwater intrusion into freshwater aquifers. Because of the compatibility produced by the mathematical model of saltwater intrusion, many researchers employ the finite element or finite volume method to arrive at the outcome. In this paper, we proposed to develop a mathematical analysis to solve the mathematical model describing the saltwater intrusion phenomenon using the radial basis function collocation method, which is a mesh-free technique for numerical solving. The simplified version of the problem has been taken into consideration. We constructed the RBF scheme and employed Newton's technique to solve the nonlinear system of equations it generated, as long as the RBF approach makes use of simply distributed nodes. The RBF scheme obtained is robust and requires knowledge of the computer programming language.

**Keywords:** saltwater intrusion; radial basis function; RBF collocation method; Newton Raphson method; Crank-Nicolson scheme.

**2020 AMS Subject Classification:** 49M15.

*Corresponding author

E-mail address: cordy2018@yahoo.com

Received July 25, 2023

## 1. INTRODUCTION

Coastal aquifers are important water resources for the population in coastal areas with high population densities and intense agricultural activity. These are areas where the demand for water is growing. This is facilitated by the shallowness of groundwater in these coastal areas. However, the exploitation of these aquifers poses complex problems because it combines the notion of groundwater reserves with that of their quality.

Of all the water on earth, only 3% of the world's water is freshwater, $2/3$ of the freshwater is frozen, forming polar ice caps, glaciers, and icebergs and $1/3$ is either surface water (found in rivers, creeks, lakes and reservoirs) or groundwater [8]. Many parts of the continent use groundwater to satisfy the daily needs of households, industry, and agriculture. Several studies have shown the risks of degradation of the quality of these slicks due to overexploitation. In the case of coastal aquifers, saltwater is denser than freshwater therefore it sinks and when the water table elevation is too low, it causes salt water to flow into the freshwater aquifers and this process is called saltwater intrusion. Human activities such as clearing land for irrigation, industrial use, etc are the main sources that increase saltwater intrusion. Then, salt effects can result in the degradation of soils and vegetation. This phenomenon requires permanent control of the use of these aquifers.

The Saltwater intrusion modeling in coastal aquifers is mainly focused on freshwater-seawater interface behavior. The interface is studied by using two assumptions; sharp form and transition zone. The following is a brief of literature review of the basic idea of the density-dependent flow of groundwater in coastal environments; the existing numerical code; and some related published results from prior works of the numerical simulation of groundwater behavior at coastal aquifers. [7] have developed some flow and transport equations adopted by FEFLOW and applied them to examine saltwater intrusion in the coastal Pingtung aquifer in southwest Taiwan, East Asia. The model can examine the lag between precipitation, surface water, and groundwater recharge. The model can also choose the best location to apply artificial recharge as a management scenario to mitigate the effect of seawater intrusion (SWI) based on the analysis of potential river flooding and maximum river flow. The results provide new hydrological insights for the region, such as the fact that the rainfall ratio between the rainy season and

the dry season in this plain is significantly higher than in the rest of Taiwan. [1] examined the displacement of the sharp boundary between saltwater and freshwater in groundwater flow, the author constructs a completely implicit finite volume approach to solve the coupled system that models seawater intrusion. The simulation was run using the open-source platform DuMu X, and numerical results from a practical test, scenarios were provided to demonstrate the method's efficiency and performance. [2] determined hydraulic heads and predicts the position of the seawater intrusion interface in the coastal aquifer of Hersonissos, near Heraklion, Crete, Greece. The simulation findings, which were obtained using the MODFLOW and SWI2 packages, demonstrate that the optimization of the pumping rates of the saltwater supply and extraction wells was more acute in some areas, such as where the thickness of the intrusion zone is shown. [4] presented a numerical model based on the Meshfree method to study the seawater intrusion problem. To simulate the seawater intrusion problem, they proposed the point collocation method (PCM) based on the radial basis function. A diffusive interface approach with density-dependent dispersion and solution flow and solute transport was used to develop the model. The model developed was verified with Henry's problem and found to be satisfactory. Furthermore, the model has been applied to another established problem and an attempt is made to examine the influence of important system parameters including pumping and recharge on seawater intrusion. [12] worked on the modeling of saline intrusion in the Tripoli-Lebanon aquifer. In this study, a Mathematical model of seawater intrusion in the Tripoli aquifer is developed, based on the implementation of the steep interface approach in " Freefem ++ ". This model mainly provides the depth of the freshwater/saltwater interface. The limitations of the model are exposed and the model is validated against the analytic solution, against the numerical code "BFSWIM " and against terrain measurements where the root mean square error varies between 0.1 $m$ and 2 $m$. [10] presented a three-dimensional density-dependent numerical model developed with FEFLOW code and model calibration, using reported water points and chloride concentrations, based on data from 14 monitored boreholes from May 2008. In December 2009, model results show that tidal-induced seawater irritation significantly affects groundwater levels and concentrations near the estuary of the Dasha River, which implies an important

hydraulic connection between this river and groundwater. The model is calibrated to predict future changes in water levels and chloride concentration. The numerical results show a decrease in the tendency for seawater intrusion if the groundwater exploitation does not reach the upper limit of about $1.32 \times 10^4 m^3/d$. The model results also guide the control of seawater intrusion in these coastal aquifer systems.

In most of the studies mentioned above, the authors modeled saltwater intrusion in different regions of the world while relying on the advection and dispersion approach and sharp interface approach. Each study uses different digital software: SUTRA, Opengeosystem, SEAWAT, MOCDESD3D, and Freefem ++. The models are validated and calibrated and have as output the concentration of salt and the hydraulic head. The results found are very interesting for developing a sustainable water consumption strategy. Since the majority of the previous work is based on steady state, the objective of this paper was to develop the mathematical analysis of the resolution of saltwater intrusion in heterogeneous and isotropic confined aquifer in an unsteady state.

Furthermore, most numerical techniques, such as the Finite Element Method, Finite Difference Method, and Finite Volume Method [5, 11], which are used to solve the mathematical model that simulates the behavior of saltwater intrusion in the literature so far, always involve mesh, or an assemblage of elements, which makes interpolation easier. The work required to build such a mesh and its connectivity data, or how each node is connected to other nodes in an interpolation scheme, and how each element shares the common nodes with other elements, is not straightforward in a complicated solution geometry. We used the RBF collocation method to improve transport simulation within the transition zone and this method is briefly presented by [3], in fact, it is a meshless method that is also simple to use theoretically and doesn't require connection data and the implementation is simple.

## 2. Differential Equations for the Mathematical Model

The model is essentially based on the coupling of two laws: the first being that which characterizes the flow velocity of a fluid in porous media, the second being that expresses the mass conservation principle [8].

**2.1. Mathematical model based on Variable density and dispersion model.** Basically, the mathematical model based on Variable density and dispersion model describing seawater intrusion in a coastal aquifer consists of:

- **•:** A definition of the geometry of the surfaces that bound the domain.
- **•:** Mass balance equation for the water(=salt solution).
- **•:** Flux equation(e.g. Darcy's law) for the water.
- **•:** Mass balance equation for the dissolved salts.
- **•:** Flux equation for the dissolved salts.
- **•:** Initial conditions that describe the known state of the system at some initial time.
- **•:** Initial conditions that describe the interaction of the domain with its environment(i.e, outside the delineated domain) across their common boundaries.

**2.2. Darcy's law.** Discovered experimentally by Darcy in 1856, Darcy's law is an equation that describes the flow of a fluid through a porous medium.It is used to define the relation between specific flow and hydraulic head which can be measured.

$$\mathbf{v} = -K\nabla h \tag{1}$$

Where: $\mathbf{v}$ denotes specific discharge (volume of fluid per unit cross-sectional area of porous medium per unit time, $m/s$) and also call as Darcy velocity.

$K$ is hydraulic conductivity or permeability $(m/s)$, and considered as isotropic, i.e. constant in all directions $x, y, z$.

$\nabla h$ is the hydraulic gradient, which is the driving force of groundwater flow per unit weight of groundwater (dimensionless).

The equation (1) is a simplified form of general physical law for fluid flow in a porous medium, which also applies to variable-density fluids [8]

$$\mathbf{v} = -\frac{k}{\mu}(\nabla P - \rho\mathbf{g}) \tag{2}$$

Where $k$ is the permeabilities $(m^2)$, a property of the porous medium; $\mu$ is dynamic viscosity $(kg/m/s)$ of the groundwater; $P$ is fluid pressure $(kg/m/s^2)$, $\rho$ is fluid density $(kg/m^3)$ and $\mathbf{g}$ is the gravitational acceleration $(m/s^2)$.

**2.3. Continuity equation or the mass balance equation for the fluid.** The continuity equation of the flow in porous media is based on the mass conservation principle and is written:

$$\frac{\partial \rho \phi}{\partial t} + div(\rho \mathbf{v}) = \rho Q \tag{3}$$

Where $\rho$ is the density of fluide ($ML^{-3}$), $\phi$ the porosity of the medium (dimensionless) and $Q$ the source term ($T^{-1}$), which express the recharge and pumping rates per unit volume of the aquifer medium.

**2.4. The mass balance equation for the dissolved salts.** The hydrodynamic dispersion equation or the mass balance equation for salt ions can be written as

$$\frac{\partial \phi C}{\partial t} = -\nabla \cdot (\mathbf{v}C - \phi D \cdot \nabla C) + CQ \tag{4}$$

Where $\phi$ is the porosity of the medium, $C$ is the concentration, $D$ is the hydrodynamic dispersion tensor, $\mathbf{v}$ Darcy flux and $Q$ source term.

**2.5. Flux equation for the dissolved salts.** The flux equation for the dissolved salts is given by [8]:

$$D_{ij} = \alpha_{ijkm} \frac{\overline{v_k}\,\overline{v_m}}{\overline{v}} f(P_e, \delta), \tag{5}$$

where $\overline{v}$ is the average velocity, $\delta$ is the ratio of the length characterizing their cross-section, and $f(P_e, \delta)$ is a function which introduces the effect of tracer transfer by molecular diffusion between adjacent streamlines at the microscopic level. For practical applications the function $f(P_e, \delta) = 1$.

**2.6. Mathematical model.** A set of four connected nonlinear partial differential equations is used to represent the seawater intrusion problem as it evolves and for the sake of simplicity, we consider the model simplified problem developed by [6] as follows:

$$S_s \frac{\partial h}{\partial t} = \nabla \cdot [K(\nabla h + \eta c \nabla z)] \tag{6}$$

$$\phi \frac{\partial c}{\partial t} = \nabla \cdot (\phi D \cdot \nabla c) - \nabla \cdot (c\mathbf{v}) \tag{7}$$

$$\mathbf{v} = -K(\nabla h + \eta c \nabla z) \tag{8}$$

$$D_{xx} = \alpha_L \frac{v_x^2}{|v|} + \alpha_T \frac{v_z^2}{|v|} + \tau D_m, D_{zz} = \alpha_T \frac{v_x^2}{|v|} + \alpha_L \frac{v_z^2}{|v|} + \tau D_m, D_{xz} = D_{zx} = (\alpha_L - \alpha_T) \frac{v_x v_z}{|v|} \tag{9}$$

where $\alpha_L$ and $\alpha_T$ are respectively the longitudinal and transverse dispersivities, $D_m$ is the molecular diffusion coefficient, $\tau$ is the tortuosity.

Now, we have

$$K(\nabla h + \eta C \nabla z) = \begin{pmatrix} K_{xx} \dfrac{\partial h}{\partial x} \\ \\ K_{zz} \left( \dfrac{\partial h}{\partial z} + \eta C \right) \end{pmatrix}, \tag{10}$$

Substituting equation (10) into the equation (8), then the equation (8) becomes

$$\mathbf{v} = \begin{pmatrix} -K_{xx} \dfrac{\partial h}{\partial x} \\ \\ -K_{zz} \left( \dfrac{\partial h}{\partial z} + \eta C \right) \end{pmatrix}, \tag{11}$$

and we obtain

$$\nabla \cdot [K(\nabla h + \eta C \nabla z)] = K_{xx} \frac{\partial^2 h}{\partial x^2} + K_{zz} \left( \frac{\partial^2 h}{\partial z^2} + \eta \frac{\partial C}{\partial z} \right). \tag{12}$$

For the sake of simplicity, we have taken the porosity $\phi$ as a constant, we then have for the transport equation,

$$\nabla \cdot (c\mathbf{v}) = -K_{xx} \frac{\partial h}{\partial x} . \frac{\partial c}{\partial x} - K_{zz} \frac{\partial h}{\partial z} . \frac{\partial c}{\partial z} - 2K_{zz} \eta c \frac{\partial c}{\partial z} - K_{xx} c \frac{\partial^2 h}{\partial x^2} - K_{zz} c \frac{\partial^2 h}{\partial z^2}, \tag{13}$$

and

$$D \cdot \nabla c = \begin{pmatrix} D_{xx} \dfrac{\partial c}{\partial x} + D_{xz} \dfrac{\partial c}{\partial z} \\ D_{zx} \dfrac{\partial c}{\partial x} + D_{zz} \dfrac{\partial c}{\partial z} \end{pmatrix}, \tag{14}$$

also,

$$\nabla \cdot (D \cdot \nabla C) = D_{xx} \frac{\partial^2 C}{\partial x^2} + D_{xz} \frac{\partial^2 C}{\partial x \partial z} + D_{zx} \frac{\partial^2 C}{\partial z \partial x} + D_{zz} \frac{\partial^2 C}{\partial z^2}. \tag{15}$$

Substituting the equation (12) into the equation (6), yields

$$\frac{\partial h}{\partial t} = \frac{1}{S_s} K_{xx} \frac{\partial^2 h}{\partial x^2} + \frac{1}{S_s} K_{zz} \frac{\partial^2 h}{\partial z^2} + \frac{1}{S_s} K_{zz} \eta \frac{\partial C}{\partial z} \tag{16}$$

Similarly, substituting the equations (13) and (15) into the equation (7) yields

$$\frac{\partial c}{\partial t} = D_{xx}\frac{\partial^2 c}{\partial x^2} + D_{xz}\frac{\partial^2 c}{\partial x \partial z} + D_{zx}\frac{\partial^2 c}{\partial z \partial x} + D_{zz}\frac{\partial^2 c}{\partial z^2} + \frac{1}{\phi}\left[K_{xx}\frac{\partial h}{\partial x}.\frac{\partial c}{\partial x} + K_{zz}\left(\frac{\partial h}{\partial z} + \eta c\right)\frac{\partial c}{\partial z}\right] + \frac{1}{\phi}\left[\left(K_{xx}\frac{\partial^2 h}{\partial x^2} + K_{zz}\frac{\partial^2 h}{\partial z^2} + K_{zz}\eta\frac{\partial c}{\partial z}\right)c\right] \tag{17}$$

## 3. Boundary Conditions

For resolution of problem (16-17), we treated the case of constant dispersion [9] where $\alpha_L = \alpha_T = 0$ and $D_m = 6,6 \cdot 10^{-2}$, $K_{xx} = K_{zz} = 1$. Thus $D_{xx} = D_{zz} = \tau D_m$ and $D_{xz} = D_{zx} = 0$. with $\tau = 1$, equation $(12)$, hence the mathematical model becomes

$$\begin{cases} \dfrac{\partial h}{\partial t} = \dfrac{1}{S_s}\Delta h + \dfrac{1}{S_s}\eta\dfrac{\partial c}{\partial z} \\ \dfrac{\partial c}{\partial t} = D_m \Delta C + \dfrac{1}{\phi}\dfrac{\partial h}{\partial x}.\dfrac{\partial c}{\partial x} + \dfrac{1}{\phi}\left(\dfrac{\partial h}{\partial z} + \eta c\right)\dfrac{\partial c}{\partial z} + \dfrac{1}{\phi}\left(\Delta h + \eta\dfrac{\partial c}{\partial z}\right)c \end{cases} \tag{18}$$

Considering the computational cost in time that motivates the method of the finite volumes for resolution of the problem 18 as in [11], Henry's problem provides the enforced boundary conditions [9]. We used the RBF Collocation method for solving the problem, compare the obtained numerical results with those discovered by the authors cited above, and then validate our test on this model.

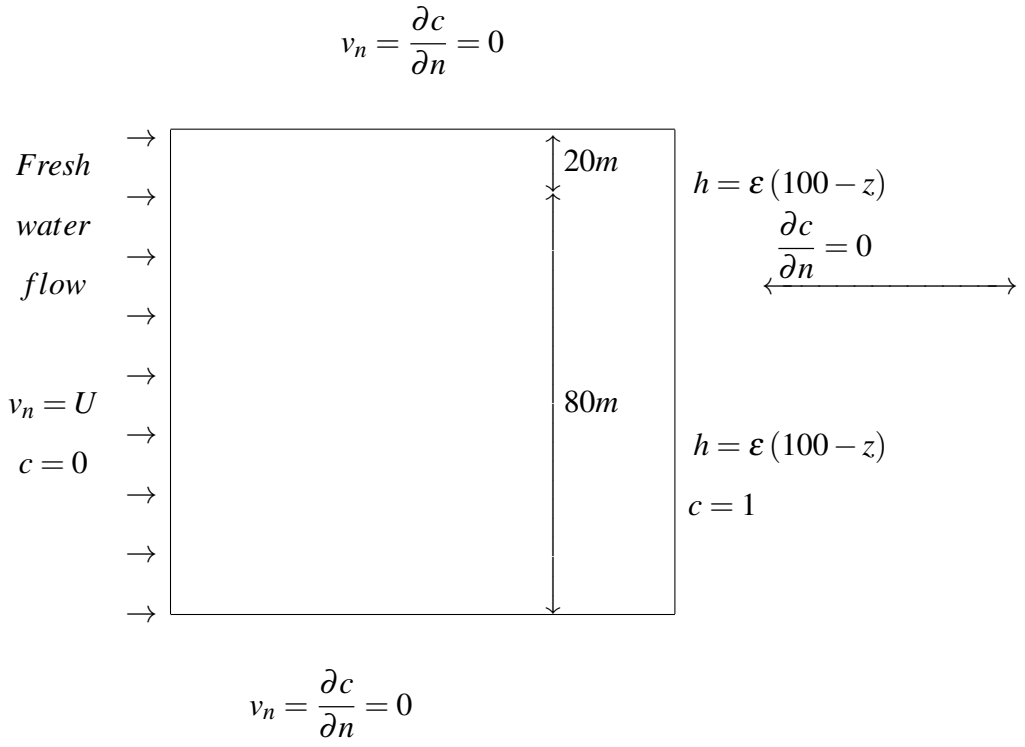


Figure 1: Henry's problem configuration

## 4. NUMERICAL TECHNIQUE

We establish a vector field $\mathbf{U} = (h, c)^t$ and the operators $L_1$, $L_2$, $L_3$, $L_4$, $\mathbf{L}$, and $\mathbf{R}$, then use it to apply the RBF Collocation method developed by [3].

$$L_1 : h \longmapsto \frac{1}{S_s}\Delta h, \tag{19}$$

$$L_2 : c \longmapsto \frac{1}{S_s}\eta\frac{\partial c}{\partial z}, \tag{20}$$

$$L_3 : h \longmapsto 0, \tag{21}$$

$$L_4 : c \longmapsto D_m \Delta c, \tag{22}$$

$$L : (h, c) \longmapsto \begin{pmatrix} L_1(h) + L_2(c) \\ \\ L_3(h) + L_4(c) \end{pmatrix} \tag{23}$$

$$\mathbf{R}:(h,c)\longmapsto\begin{pmatrix}R_1(h,c)\\ \\ R_2(h,c)\end{pmatrix}=\begin{pmatrix}0\\ \\ \frac{1}{\phi}\frac{\partial h}{\partial x}.\frac{\partial c}{\partial x}+\frac{1}{\phi}\left(\frac{\partial h}{\partial z}+\eta c\right)\frac{\partial c}{\partial z}+\frac{1}{\phi}\left(\Delta h+\eta\frac{\partial c}{\partial z}\right)c\end{pmatrix}. \tag{24}$$

Substituting the equations (19),(20),(21),(22),(23) and (24) into the equation (18), we then obtain

$$\begin{cases}\dfrac{\partial h}{\partial t}=L_1(h)+L_2(c)\\ \\ \dfrac{\partial c}{\partial t}=L_4(c)+R_2(h,c)\end{cases} \tag{25}$$

where $R_2(h,c)=\frac{1}{\phi}\frac{\partial h}{\partial x}.\frac{\partial c}{\partial x}+\frac{1}{\phi}\left(\frac{\partial h}{\partial z}+\eta c\right)\frac{\partial c}{\partial z}+\frac{1}{\phi}\left(\Delta h+\eta\frac{\partial c}{\partial z}\right)c$

Thus, the problem 25 can be written as:

$$\begin{cases}\dfrac{\partial \mathbf{U}}{\partial t}=\mathbf{L}\cdot\mathbf{U}+\mathbf{R}(\mathbf{U}) \quad on \quad [0,200]\times[0,100]\times[0,T[\\ \\ \mathbf{U}(\mathbf{x},0)=\mathbf{0} \qquad \forall \mathbf{x}\in[0,200]\times[0,100]\end{cases} \tag{26}$$

With $T$ is the maximum convergence time for the problem-solving algorithm.

In order to discretize problem 26, we applied the iterative Newton technique established in [3], the Crank-Nicolson scheme, and the RBF Collocation approach.

$$\begin{cases}\dfrac{\mathbf{U}^{n+1}-\mathbf{U}^n}{\Delta t}=\dfrac{1}{2}\left(\mathbf{L}\cdot\mathbf{U}^{n+1}+\mathbf{R}\left(\mathbf{U}^{n+1}\right)\right)+\dfrac{1}{2}\left(\mathbf{L}\cdot\mathbf{U}^n+\mathbf{R}(\mathbf{U}^n)\right) \quad on \quad [0,200]\times[0,100]\\ \\ \mathbf{U}^0(x,z)=\mathbf{U}(x,z,0)=\mathbf{0} \qquad \forall (x,z)\in[0,200]\times[0,100]\end{cases} \tag{27}$$

where $\mathbf{U}^n(x,z)\approx\mathbf{U}(x,z,t_n)$ is the approximation of the solution at $t_n=n\Delta t$, and $\Delta t=t_{n+1}-t_n$ is the time step.

RBF Collocation method assumes that the field of the unknown vector $\mathbf{U}=(h,c)$, that is, $\mathbf{U}(x,z,t)=(h(x,z,t),c(x,z,t))$ with $h(x,z,t)=\sum_{j=0}^{N-1}h_j(t)\psi_j(x,z)$, $c(x,z,t)=\sum_{j=0}^{N-1}c_j(t)\psi_j(x,z)$

where $\left(\psi_j\right)_{0\le j\le N-1}$ are given functions

$\psi_j : \mathbb{R}^2 \longrightarrow \mathbb{R}$ $\quad (x,z) \longmapsto \psi\left(\left\|(x,z)-(x_j,z_j)\right\|_2\right)$, $(x_j,z_j)_{0\le j\le N-1}$ are $N$ points set in $[0,200]\times[0,100]$, $\psi$ is a fixed radial function, and $\|.\|_2$ is the Euclidean norm of $\mathbb{R}^2$.

We set $\mathbf{U}^n(x,z)=\mathbf{U}(x,z,t_n)$, $h^n(x,z)=h(x,z,t_n)$ , $c^n(x,z)=c(x,z,t_n)$, then $h_j^n=h_j(t_n)$ and $c_j^n=c_j(t_n)$.

Thus, we have

$$\mathbf{U}^n(x,z)=\begin{pmatrix}\sum_{j=0}^{N-1} h_j^n\psi_j(x,z)\\ \\ \sum_{j=0}^{N-1} c_j^n\psi_j(x,z)\end{pmatrix}. \tag{28}$$

Equation (27) is transformed into

$$\begin{cases}\mathbf{U}^{n+1}-\dfrac{1}{2}\Delta t\left[\mathbf{L}\cdot\mathbf{U}^{n+1}+\mathbf{R}\left(\mathbf{U}^{n+1}\right)\right]=\mathbf{U}^n+\dfrac{1}{2}\Delta t\left[\mathbf{L}\cdot\mathbf{U}^n+\mathbf{R}\left(\mathbf{U}^n\right)\right]\\ \\ \mathbf{U}^0=\mathbf{L}\cdot\mathbf{U}^0=\mathbf{R}\left(\mathbf{U}^0\right)=\mathbf{0}\end{cases} \tag{29}$$

By reccurrence we show that

$$\mathbf{U}^{n+1}-\frac{1}{2}\Delta t\left[\mathbf{L}\cdot\mathbf{U}^{n+1}+\mathbf{R}\left(\mathbf{U}^{n+1}\right)\right]=2(-1)^n\sum_{k=0}^{n}(-1)^k\mathbf{U}^k, \tag{30}$$

we finally obtain the following scheme

$$\begin{cases}\sum_{j=0}^{N-1} h_j^{n+1}\left(\psi_j-\dfrac{1}{2S_s}\Delta t\Delta\psi_j\right)+\sum_{j=0}^{N-1} c_j^{n+1}\left(-\dfrac{1}{2S_s}\eta\Delta t\right)\dfrac{\partial\psi_j}{\partial z}=2(-1)^n\sum_{k=0}^{n}(-1)^k h^k\\ \\ \sum_{j=0}^{N-1} c_j^{n+1}\left(\psi_j-\dfrac{1}{2}\Delta t D_m\Delta\psi_j\right)-\dfrac{1}{2}\Delta t R_2\left(h^{n+1},c^{n+1}\right)=2(-1)^n\sum_{k=0}^{n}(-1)^k c^k\end{cases} \tag{31}$$

**4.1. Newton Raphson method for a system of nonlinear equations (31).** For solving nonlinear systems of equations (31), the Newton-Raphson method is the preferred approach.

We set

$$\zeta^{n+1}=\left(\zeta_j^{n+1}\right),\ 0\le j\le 2N-1 \text{ with } \begin{cases}\zeta_j^{n+1}=h_j^{n+1},\ \text{if } 0\le j\le N-1\\ \zeta_j^{n+1}=c_{j-N}^{n+1},\ \text{if } N\le j\le 2N-1\end{cases} \tag{32}$$

$$\begin{cases} \chi_j = \psi_j - \dfrac{\Delta t}{2S_s}\Delta\psi_j, \text{ if } 0 \leq j \leq N-1 \\ \chi_j = \left(-\dfrac{1}{2S_s}\eta\Delta t\right)\dfrac{\partial \psi_{j-N}}{\partial z}, \text{ if } N \leq j \leq 2N-1 \end{cases} \tag{33}$$

Furthermore, we have

$$\widetilde{F_1}\left(\zeta^{n+1}\right) = \sum_{j=0}^{N-1} h_j^{n+1}\left(\psi_j - \frac{\Delta t}{2S_s}\Delta\psi_j\right) + \sum_{j=0}^{N-1} c_j^{n+1}\left(-\frac{1}{2S_s}\eta\Delta t\right)\frac{\partial \psi_j}{\partial z}, \tag{34}$$

then

$$\widetilde{F_1}\left(\zeta^{n+1}\right) = \sum_{j=0}^{N-1} h_j^{n+1}\left(\psi_j - \frac{\Delta t}{2S_s}\Delta\psi_j\right) + \sum_{j=N}^{2N-1} c_{j-N}^{n+1}\left(-\frac{1}{2S_s}\eta\Delta t\right)\frac{\partial \psi_{j-N}}{\partial z} \tag{35}$$

which implies that,

$$\widetilde{F_1}\left(\zeta^{n+1}\right) = \sum_{j=0}^{2N-1} \zeta_j^{n+1}\chi_j \tag{36}$$

$$W_1^n = 2(-1)^n \sum_{k=0}^{n} (-1)^k h^k. \tag{37}$$

Similarly, we have

$$\widetilde{G_1}\left(\zeta^{n+1}\right) = \sum_{j=0}^{N-1} c_j^{n+1}\left(\psi_j - \frac{1}{2}\Delta t D_m \Delta\psi_j\right) - \frac{1}{2}\Delta t R_2\left(h^{n+1}, c^{n+1}\right) \tag{38}$$

$$W_2^n = 2(-1)^n \sum_{k=0}^{n} (-1)^k c^k \tag{39}$$

Hence, for $(x_i, z_i) \in [0,200] \times [0,100]$ , $0 \leq i \leq N-1$, we have

$$\begin{cases} \widetilde{F_1}\left(\zeta^{n+1}\right)(x_i,z_i) = \sum\limits_{j=0}^{2N-1} \zeta_j^{n+1}\chi_j(x_i,z_i) \\ \widetilde{G_1}\left(\zeta^{n+1}\right)(x_i,z_i) = \sum\limits_{j=0}^{N-1} C_j^{n+1}\left(\psi_j(x_i,z_i) - \dfrac{1}{2}\Delta t D_m \Delta\psi_j(x_i,z_i)\right) - \dfrac{1}{2}\Delta t R_2\left(h^{n+1}, c^{n+1}\right)(x_i,z_i) \end{cases} \tag{40}$$

$$\begin{cases} \widetilde{F_1}\left(\zeta^{n+1}\right)(x_i,z_i) - W_1^n(x_i,z_i) = 0,\ 0 \leq i \leq N-1 \\ \widetilde{G_1}\left(\zeta^{n+1}\right)(x_i,z_i) - W_2^n(x_i,z_i) = 0, 0 \leq i \leq N-1 \end{cases} \tag{41}$$

Let

$$L=(F,G) \text{ with } \begin{cases} F &= (F_i)_{0\le i\le N-1} \\ G &= (G_i)_{N\le i\le 2N-1} \end{cases} \tag{42}$$

$$F\left(\zeta^{n+1}\right)=\left(F_i\left(\zeta^{n+1}\right)\right)_{0\le i\le N-1} \tag{43}$$

$$G\left(\zeta^{n+1}\right)=\left(G_i\left(\zeta^{n+1}\right)\right)_{N\le i\le 2N-1} \tag{44}$$

where

$$F_i\left(\zeta^{n+1}\right)=\widetilde{F_1}\left(\zeta^{n+1}\right)(x_i,z_i)-W_1^n(x_i,z_i),\ 0\le i\le N-1 \tag{45}$$

$$G_i\left(\zeta^{n+1}\right)=\widetilde{G_1}\left(\zeta^{n+1}\right)(x_{i-N},z_{i-N})-W_2^n(x_{i-N},z_{i-N}),\ N\le i\le 2N-1 \tag{46}$$

$L=(F,G)$ can be now written as

$$L=(L_i)_{0\le i\le 2N-1} \text{ with } \begin{cases} L_i &= F_i \ if\ 0\le i\le N-1 \\ L_i &= G_i \ if\ N\le i\le 2N-1 \end{cases} \tag{47}$$

We then obtain

$$L\left(\zeta^{n+1}\right)=\left(L_i\left(\zeta^{n+1}\right)\right)_{0\le i\le 2N-1}. \tag{48}$$

The Jacobian matrix of the operator $L$ at $\zeta^{n+1}$ is therefore written

$$JL\left(\zeta^{n+1}\right)=\left(\frac{\partial L_i}{\partial \zeta_j^{n+1}}\left(\zeta^{n+1}\right)\right)_{\substack{0\le i\le 2N-1\\ 0\le j\le 2N-1}} \tag{49}$$

$$\frac{\partial L_i}{\partial \zeta_j^{n+1}}\left(\zeta^{n+1}\right)=\frac{\partial F_i}{\partial h_j^{n+1}}\left(\zeta^{n+1}\right),\ 0\le i\le N-1,\ 0\le j\le N-1, \tag{50}$$

$$\frac{\partial L_i}{\partial \zeta_j^{n+1}}\left(\zeta^{n+1}\right)=\frac{\partial F_i}{\partial c_{j-N}^{n+1}}\left(\zeta^{n+1}\right),\ 0\le i\le N-1,\ N\le j\le 2N-1, \tag{51}$$

$$\frac{\partial L_i}{\partial \zeta_j^{n+1}}\left(\zeta^{n+1}\right)=\frac{\partial G_i}{\partial h_j^{n+1}}\left(\zeta^{n+1}\right),\ N\le i\le 2N-1,\ 0\le j\le N-1, \tag{52}$$

$$\frac{\partial L_i}{\partial \zeta_j^{n+1}}\left(\zeta^{n+1}\right)=\frac{\partial G_i}{\partial c_{j-N}^{n+1}}\left(\zeta^{n+1}\right),\ N\le i\le 2N-1,\ N\le j\le 2N-1, \tag{53}$$

Let's now calculate (50), (51), (52), (52) and (53). By deriving (45) and (46) with respect to the variables $h_j^{n+1}$ and $c_j^{n+1}$, we then get

$$\frac{\partial L_i}{\partial \zeta_j^{n+1}}\left(\zeta^{n+1}\right) = \frac{\partial F_i}{\partial h_j^{n+1}}\left(\zeta^{n+1}\right) = \chi_j\left(x_i,z_i\right) = \psi_j\left(x_i,z_i\right) - \frac{1}{2}\frac{\Delta t}{S_s}\Delta\psi_j\left(x_i,z_i\right), \tag{54}$$
$$0 \le i \le N-1, 0 \le j \le N-1$$

$$\frac{\partial L_i}{\partial \zeta_j^{n+1}}\left(\zeta^{n+1}\right) = \frac{\partial F_i}{\partial C_{j-N}^{n+1}}\left(\zeta^{n+1}\right) = \chi_j\left(x_i,z_i\right) = -\frac{1}{2}\frac{\eta\Delta t}{S_s}\frac{\partial \psi_{j-N}}{\partial z}\left(x_i,z_i\right), \tag{55}$$
$$0 \le i \le N-1, N \le j \le 2N-1$$

$$\frac{\partial L_i}{\partial \zeta_j^{n+1}}\left(\zeta^{n+1}\right) = \frac{\partial G_i}{\partial h_j^{n+1}}\left(\zeta^{n+1}\right) = -\frac{1}{2}\Delta t\frac{\partial R_2}{\partial h_j^{n+1}}\left(h^{n+1},c^{n+1}\right)\left(x_{i-N},z_{i-N}\right) = 0, \tag{56}$$
$$N \le i \le 2N-1, 0 \le j \le N-1$$

$$\begin{aligned}\frac{\partial L_i}{\partial \zeta_j^{n+1}}\left(\zeta^{n+1}\right) = \frac{\partial G_i}{\partial C_{j-N}^{n+1}}\left(\zeta^{n+1}\right) &= \psi_{j-N}\left(x_{i-N},z_{i-N}\right) - \frac{1}{2}\Delta t D_m \Delta\psi_{j-N}\left(x_{i-N},z_{i-N}\right) \\ &-\frac{1}{2}\Delta t\frac{\partial R_2}{\partial c_{j-N}^{n+1}}\left(h^{n+1},c^{n+1}\right)\left(x_{i-N},z_{i-N}\right), N \le i \le 2N-1, N \le j \le 2N-1\end{aligned} \tag{57}$$

For $X^0$ given, we construct a sequence $\left(X^k\right)$ such that $X^k = \left(X_j^k\right)_{0\le j\le 2N-1}$

with
$$\begin{aligned} X_j^k &= h_j^{k+1}, if\ 0 \le j \le N-1 \\ X_j^k &= C_{j-N}^{k+1}, if\ N \le j \le 2N-1\end{aligned}$$

The Newton system is given by

$$X^{k+1} = X^k - \left[J_{\left(X^k\right)}(L)\right]^{-1}\cdot L\left(X^k\right) \tag{58}$$

where $J_{\left(X^k\right)}(L) = \left(\frac{\partial L_i}{\partial X_j^k}\left(X^k\right)\right)_{\substack{0\le i\le 2N-1\\ 0\le j\le 2N-1}}$ is the Jacobian matrix of operator $L$ in $X^k$ which is equivalent to solving

$$\begin{cases} \left[J_{\left(X^k\right)}(L)\right]\cdot Z^k = -L\left(X^k\right) \\ X^{k+1} = X^k + Z^k \text{ until } \left\|Z^k\right\|_2 \prec \delta \text{ with } \delta \prec\prec 1 \text{ previously fixed}\end{cases} \tag{59}$$

**4.2. Boundary condition discretization.** With the relation $V = -K(\nabla h + \eta C \nabla z)$ and $K = \begin{pmatrix} 1 & 0 \\ 0 & 1 \end{pmatrix}$, we have $\mathbf{v} = \begin{pmatrix} v_x \\ v_z \end{pmatrix}$ with $v_x = -\dfrac{\partial h}{\partial x}$ and $v_z = -\left(\dfrac{\partial h}{\partial z} + \eta c\right)$ from the equation (11).

**4.2.1.** *West boundary.* $v_x = U$, $c = 0$. We have a boundary condition of Dirichlet type on the concentration and a Neuman type boundary condition on the hydraulic head, we have

$$
\left\{
\begin{array}{ll}
\dfrac{\partial h^{n+1}}{\partial x}(0,z) = U & \\
c^{n+1}(0,z) = 0 = 0 & \\
\dfrac{\partial c^{n+1}}{\partial z}(0,z) = 0 & \\
\dfrac{\partial^2 c^{n+1}}{\partial z^2}(0,z) = 0 & \forall z \in ]0;100[ \\
R_2\left(h^{n+1}, c^{n+1}\right)(0,z) = \dfrac{U}{\phi}\dfrac{\partial c^{n+1}}{\partial x}(0,z) & \\
\dfrac{\partial R_2}{\partial h_j^{n+1}}\left(h^{n+1}, c^{n+1}\right)(0,z) = 0 & \\
\dfrac{\partial R_2}{\partial c_j^{n+1}}\left(h^{n+1}, c^{n+1}\right)(0,z) = \dfrac{U}{\phi}\dfrac{\partial \psi_j}{\partial x}(0,z) &
\end{array}
\right. \tag{60}
$$

**4.2.2.** *South boundary.* We have a Neuman type boundary condition on the hydraulic head and the concentration $v_n = 0$ and $\dfrac{\partial c}{\partial n} = 0$. Thus,

$$
\left\{
\begin{array}{ll}
\dfrac{\partial h^{n+1}}{\partial z}(x,0) + \eta c^{n+1}(x,0) = 0 & \\
\dfrac{\partial c^{n+1}}{\partial z}(x,0) = 0 & \\
R_2\left(h^{n+1}, c^{n+1}\right)(x,0) \approx \dfrac{2}{\Delta t} c^{n+1}(x,0) - D_m \Delta c^{n+1}(x,0) - W_2^n(x,0) & \forall x \in ]0;200[ \\
\dfrac{\partial R_2}{\partial h_j^{n+1}}\left(h^{n+1}, c^{n+1}\right)(x,0) \approx 0 & \\
\dfrac{\partial R_2}{\partial c_j^{n+1}}\left(h^{n+1}, c^{n+1}\right)(x,0) \approx \dfrac{2}{\Delta t}\psi_j(x,0) - D_m \Delta \psi_j(x,0) &
\end{array}
\right. \tag{61}
$$

**4.2.3.** *North boundary.* Similarly, we have a Neuman type boundary condition on the hydraulic head and the concentration $v_n = 0$ and $\dfrac{\partial c}{\partial n} = 0$. Thus,

$$
(62)\quad \begin{cases}
\dfrac{\partial h^{n+1}}{\partial z}(x,100) + \eta c^{n+1}(x,100) = 0 \\
\dfrac{\partial c^{n+1}}{\partial z}(x,100) = 0 \qquad\qquad (40) \\
R_2\left(h^{n+1}, c^{n+1}\right)(x,100) \approx \dfrac{2}{\Delta t} c^{n+1}(x,100) - D_m \Delta c^{n+1}(x,100) - W_2^n(x,100) \qquad \forall x \in ]0;200[ \\
\dfrac{\partial R_2}{\partial h_j^{n+1}}\left(h^{n+1}, c^{n+1}\right)(x,100) \approx 0 \\
\dfrac{\partial R_2}{\partial c_j^{n+1}}\left(h^{n+1}, c^{n+1}\right)(x,100) \approx c\dfrac{2}{\Delta t}\psi_j(x,100) - D_m \Delta \psi_j(x,100)
\end{cases}
$$

**4.2.4.** *East boundary.*

$$
(63)\quad \forall z \in ]0;80[, \begin{cases}
h^{n+1}(200,z) = \varepsilon(100 - z) \\
\dfrac{\partial h^{n+1}}{\partial z}(200,z) = -\varepsilon, \\
\dfrac{\partial^2 h^{n+1}}{\partial z^2}(200,z) = 0 \\
c^{n+1}(200,z) = 1, \\
\dfrac{\partial c^{n+1}}{\partial z}(200,z) = 0, \\
\dfrac{\partial^2 c^{n+1}}{\partial z^2}(200,z) = 0 \\
R_2\left(h^{n+1}, c^{n+1}\right)(200,z) = \dfrac{2}{\Delta t} c^{n+1}(200,z) - D_m \Delta c^{n+1}(200,z) - W_2^n(200,z) \\
\dfrac{\partial R_2}{\partial h_j^{n+1}}\left(h^{n+1}, c^{n+1}\right)(200,z) \approx 0 \\
\dfrac{\partial R_2}{\partial c_j^{n+1}}\left(h^{n+1}, c^{n+1}\right)(200,z) \approx \dfrac{2}{\Delta t}\psi_j(200,z) - D_m \Delta \psi_j(200,z)
\end{cases}
$$

**4.2.5.** *Initial conditions.*

$$\begin{cases} h^0(x,z) = h(x,z,0) = 0 \\ \qquad\qquad\qquad\qquad ,\forall (x,z) \in [0,200]\times[0,100] \\ c^0(x,z) = c(x,z,0) = 0 \end{cases} \tag{64}$$

We choose 30 nodes from the boundary $\partial\Omega$ and 36 interior nodes at $\Omega$ spacing of $20m$ . Hence, the number of nodes is N=66. The nodes $(x_i, z_i)$ are defined as follows:

$$(x_i,z_i) = (i*PAS\ ;\ 0), if\ 0 \le i \le 10 \tag{65}$$

$$(x_i,z_i) = ((i-11)*PAS\ ;\ PAS), if\ 11 \le i \le 21$$

$$(x_i,z_i) = ((i-22)*PAS\ ;\ 2*PAS), if\ 22 \le i \le 32$$

$$(x_i,z_i) = ((i-33)*PAS\ ;\ 3*PAS), if\ 33 \le i \le 43$$

$$(x_i,z_i) = ((i-44)*PAS\ ;\ 4*PAS), if\ 44 \le i \le 54$$

$$(x_i,z_i) = ((i-55)*PAS\ ;\ 5*PAS), if\ 55 \le i \le 65$$

$$(x_i,z_i) = ((i-66)*PAS\ ;\ 0), if\ 66 \le i \le 76$$

$$(x_i,z_i) = ((i-77)*PAS\ ;\ PAS), if\ 77 \le i \le 87$$

$$(x_i,z_i) = ((i-88)*PAS\ ;\ 2*PAS), if\ 88 \le i \le 98$$

$$(x_i,z_i) = ((i-99)*PAS\ ;\ 3*PAS), if\ 99 \le i \le 109$$

$$(x_i,z_i) = ((i-110)*PAS\ ;\ 4*PAS), if\ 110 \le i \le 120$$

$$(x_i,z_i) = ((i-121)*PAS\ ;\ 5*PAS), if\ 121 \le i \le 131$$

where $PAS$ means the step of subdivision of coordinate axes. We chose here $PAS = 20m$.

The hydraulics parameters $S_s$, $\phi$, $\varepsilon$, $C_{\max}$, $\eta$ are taken those from the digital experiment test of Henry's problem [9], that is to say $S_s = 0.1$, $\phi = 0,35$, $\varepsilon = 0,0245$, $c_{\max} = 1$.

## ACKNOWLEDGMENT

The authors would like to express their gratitude to the anonymous referee for meticulously checking the facts and offering insightful criticism that improved this article.

## CONFLICT OF INTERESTS

The authors declare that there is no conflict of interests.

## REFERENCES

[1] A. Aharmouch, B. Amaziane, M. El Ossmani, et al. A fully implicit finite volume scheme for a seawater intrusion problem in coastal aquifers, Water. 12 (2020), 1639.

[2] A. Pappa, Z. Dokou, G.P. Karatzas, Saltwater intrusion management using the SWI2 model: application in the coastal aquifer of Hersonissos, Crete, Greece, Desal. Water Treat. 99 (2017), 49–58.

[3] A.F. Ouassissou, C. Tathy, Application of the RBF collocation method to solve the classic problem of a meson field, Far East J. Appl. Math. 84 (2013), 37.

[4] A. Thomas, T.I. Eldho, A.K. Rastogi, Simulation of Seawater intrusion in coastal confined aquifer using a point collocation method based meshfree model, J. Water Resource Protect. 8 (2016), 534–549.

[5] A. AL-Bitar, Modélisation des écoulements en milieu poreux hétérogènes 2D/3D, avec couplages surface/souterain et densitaires, Thèse présentée à l' université de Toulouse, Ecole doctorale: Sciences de l'univers, Espace, Environnement, (2007).

[6] C.J. Itoua-Tsele, C.Tathy, D.M. Malonza, Mathematical model for three-dimensional flow in porous media for confined aquifer in mixing zone modeling to study saltwater intrusion in coastal aquifer, Int. J. Sci. Technol. Res. 9 (2020), 1261–12668.

[7] D. Mahdieh, A.J. Akbar, M. Akrami, K. Kai-Yuan, et al. Coupled three-dimensional modelling of groundwater-surface water interactions for management of seawater intrusion in Pingtung Plain, Taiwan, J. Hydrol.: Region. Stud. 36 (2021), 100850.

[8] J. Bear, Modeling phenomena of flow and transport in porous media, Cham: Springer International Publishing, (2018).

[9] H.R. Henry, Effects of dispersion on salt encroachment in coastal aquifers, in" Seawater in Coastal Aquifers, US Geological Survey, Water Supply Paper, 1613 (1964), pp. C70-C80.

[10] W. Lu, Q. Yang, J.D. Martín, et al. Numerical modelling of seawater intrusion in Shenzhen (China) using a 3D density-dependent model including tidal effects, J. Earth System Sci. 122 (2013), 451-465.

[11] M. Hamidi, S. Reza, S. Yazdi, Numerical modeling of seawater intrusion in coastal aquifer using finite volume unstructured mesh method, WSEAS Trans. Math. 5 (2006), 648.

[12] O. Kalaoun, Modélisation de l'intrusion saline dans l'aquifère de Tripoli-Liban: impact des changements globaux, PhD thesis, Université de Toulouse III-Paul Sabatier, France, (2015).